ONLINE SECONDARY PATH MODELLING IN WAVE-DOMAIN ACTIVE NOISE CONTROL

Wen Zhang[1], *Christian Hofmann*[2], *Michael Bürger*[2], *Thushara Abhayapala*[1], *and Walter Kellermann*[2]

[1]Research School of Engineering, College of Engineering and Computer Science
The Australian National University, Canberra, ACT 0200, Australia
{wen.zhang, thushara.abhayapala}@anu.edu.au
[2]Multimedia Communications and Signal Processing
Friedrich-Alexander University Erlangen-Nürnberg (FAU), 91058 Erlangen, Germany
{Christian.Hofmann, Michael.Buerger, Walter.Kellermann}@FAU.de

ABSTRACT

The performance of an ANC system largely depends on the availability of an accurate secondary path model. This is however a major challenge in multichannel ANC where the computational complexity increases significantly with the number of secondary sources and error sensors. This paper proposes wave-domain adaptive processing algorithm for multichannel ANC with online secondary modelling to cancel a tonal noise over a region of space within a reverberant room. The design is based on exploiting a special property of the secondary path model in the wave domain. A feedback control system is implemented, where a single microphone array is placed at the boundary of the control region to measure the residual signals, and a loudspeaker array reproduces secondary sources to generate the anti-noise signals and auxiliary noise for secondary path modelling. Through experimental verification in comparison with existing methods the proposed algorithm demonstrates more efficient adaptation with low-level auxiliary noise.

***Index Terms*—** Active noise control, secondary path modelling, wave domain, adaptive processing, feedback system

1. INTRODUCTION

Active noise control (ANC), also known as noise cancellation, is designed based on the principle of superposition, that is, an anti-noise signal of equal amplitude and opposite phase is generated by the secondary source to cause destructive interference and to cancel the unwanted (primary) noise [1, 2]. Multichannel ANC mainly deals with a noise field over space, which requires several secondary sources and sensors, thus making it more expensive to implement. ANC system for the car interior is a typical multichannel ANC application, which is capable of reducing short-time stationary noise, such as engine noise, at frequencies up to a few hundred Hertz [3, 4].

The general multichannel ANC system using the filtered-x LMS (Least Mean Squares) algorithm was proposed in both time domain and frequency domain [5, 6, 7] with the convergence analysis provided in [8]. The computational complexity of the multichannel ANC system increases significantly with the number of secondary sources and error sensors, which represents one of the major challenges for applying multichannel ANC in large-scale applications [9]. In addition, in multichannel ANC, the noise control is achieved mainly at the error sensor positions or its close surroundings and noise still exists at other positions [10]. However, in many practical ANC applications, especially in consumer electronics and medical instruments (e.g., magnetic resonance imaging (MRI) systems and infant incubators), it is desired to create quiet zones away from error sensors.

Wave-domain signal processing, a technique commonly used for sound control over large spatial regions, has been proposed for ANC over space [10, 11]. The principle of wave-domain signal representation is to use fundamental solutions of the Helmholtz wave-equation as basis functions to express a wave field over a spatial region. Processing directly on the decomposition coefficients therefore controls sound within that region. The wave-domain ANC with feedforward [11] and feedback [10, 12] configurations have been investigated and the results show that significant noise cancellation over the entire region of interest can be achieved.

When dealing with unknown and time-varying acoustic responses between the secondary sources and error sensors (normally referred as the secondary path), adaptive filters are required to track variations. However, there are fundamental problems associated with the adaptation of the filters in the conventional time-frequency domain, such as high computational complexity and low adaptation performance [13]. Especially, due to strong mutual interference, the problem of online secondary-path modelling (SPM) in multichannel ANC has hardly been addressed and most existing work assume that the secondary path is known as a prior.

In this work, we propose an adaptive wave-domain ANC system with an effective strategy of online SPM based on the concepts already outlined in [11, 14, 15] for acoustic echo cancellation, room equalization, and ANC. The problem is defined as to cancel a tonal noise (i.e., a single frequency noise) on a 2D plane in a reverberant room, within which the secondary-path is unknown. The proposed algorithm requires low-level auxiliary noise for online SMP and also demonstrates efficient adaptation.

2. ANC IN THE WAVE DOMAIN

Assuming L loudspeaker signals $x_\ell(n)$ (secondary sources) and P microphones (error sensors), the received signals $y_p(n)$ at the microphones are written as

$$y_p(n) = \sum_{\ell=1}^{L} x_\ell(n) * h_{p\ell}(n) + d_p(n), \quad p = 1, \ldots, P \qquad (1)$$

This work is supported by Australian Research Council (ARC) Discovery Projects funding scheme (project no. DP140103412).

Wen Zhang is also with Center of Intelligent Acoustics and Immersive Communications, Northwestern Polytechnical University, Xian, Shaanxi 710072, China.

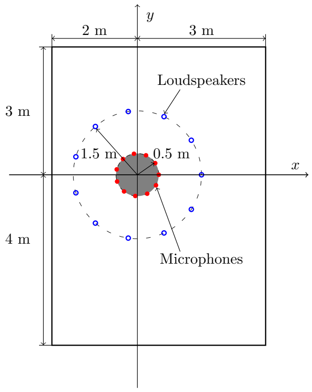

Fig. 1. System setup for a wave-domain ANC in a reverberant room. Uniform circular arrays of loudspeakers (blue) and microphones (red) are placed concentrically for noise cancellation within the shaded region.

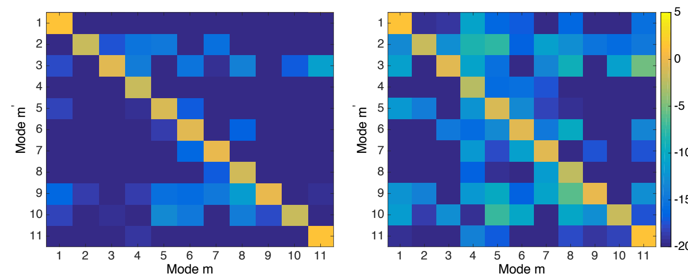

(a) (b)

Fig. 2. Plots of the wave-domain secondary path $\boldsymbol{H}_{\mathrm{w}}$ on a logarithmic scale in a 2D room of size 5×7 m with reflection coefficient and reverberation time (a) $\beta = 0.5$, $T_{60} \approx 145$ ms and (b) $\beta = 0.8$, $T_{60} \approx 300$ ms, respectively.

where $h_{p\ell}(n)$ is the secondary path from the ℓth speaker to the pth microphone, $*$ represents the time-domain convolution with respect to the time index n, and $d_p(n)$ is the recording of the primary noise at the pth microphone.

It is assumed that the secondary path is time-varying and unknown; hence, the secondary source signal does not only consist of the anti-noise signal $x_\ell^{\mathrm{c}}(n)$, but it also contains an auxiliary noise signal $x_\ell^{\mathrm{e}}(n)$ for online SPM, i.e.,

$$x_\ell(n) = x_\ell^{\mathrm{c}}(n) + x_\ell^{\mathrm{e}}(n). \tag{2}$$

It is desired to use low-level auxiliary noise so that during online SPM the overall noise inside the control region would not be too excessive.

We adopt a block-wise operation and transform the signal into the time-frequency domain to get the following representation,

$$Y_p(q, \omega) = \sum_{\ell=1}^{L} X_\ell(q, \omega) H_{p\ell}(q, \omega) + D_p(q, \omega), \tag{3}$$

where q and ω denote the qth time block and the ωth frequency component, respectively. As the ANC system is designed at a single frequency, ω is removed from the notation for conciseness of presentation. Representing (3) in matrix form gives us

$$\boldsymbol{Y}(q) = \boldsymbol{H}(q)\boldsymbol{X}(q) + \boldsymbol{D}(q). \tag{4}$$

The system is deployed on a 2D plane as shown in Fig. 1, where the loudspeakers and microphones are placed on two concentrically placed circular arrays. The wave-domain transforms after [16, 17] decompose the wave field into the expansion coefficients with respect to circular harmonics [18], which are orthogonal basis functions on a circle. Based on the microphone recordings, the received signals in the wave domain are obtained,

$$Y_{\mathrm{w}}^m(q) = \frac{1}{P} \sum_{p=1}^{P} Y_p(q) e^{-im\phi_p}, \quad m = -M_0, \ldots, M_0, \tag{5}$$

where $(\cdot)_{\mathrm{w}}$ represents the wave-domain signal and m is termed the mode; $M_0 = \lceil kr_0 \rceil$, $k = 2\pi f/c$ is the wave number, and r_0 is the radius of the microphone array.

The wave-domain transform for the secondary source signals are defined as the wave-domain signals produced by the speakers at the microphones under free-field conditions [16, 19], that is

$$X_{\mathrm{w}}^m(q) = \frac{1}{P} \sum_{p=1}^{P} \sum_{\ell=1}^{L} G_{p\ell} X_\ell(q) e^{-im\phi_p}, \quad m = -M_0, \ldots, M_0, \tag{6}$$

where $G_{p\ell}$ is the Green's function for the wave equation in 3D and used to represent the propagation of a point source in the free field [20].

We use $\boldsymbol{T}_1^{\mathrm{f}}$ and $\boldsymbol{T}_2^{\mathrm{f}}$ to denote the forward wave-domain transform for secondary source signals and received signals based on (5) and (6) [16, 21]. The backward wave-domain transform $\boldsymbol{T}_1^{\mathrm{b}}$ and $\boldsymbol{T}_2^{\mathrm{b}}$ are defined simply the inverse of the forward transform. Then, we have the same relation of (3) in the wave domain,

$$\boldsymbol{Y}_{\mathrm{w}}(q) = \boldsymbol{H}_{\mathrm{w}}(q)\boldsymbol{X}_{\mathrm{w}}(q) + \boldsymbol{D}_{\mathrm{w}}(q), \tag{7}$$

where $\boldsymbol{Y}_{\mathrm{w}} = \boldsymbol{T}_2^{\mathrm{f}}\boldsymbol{Y}$, $\boldsymbol{D}_{\mathrm{w}} = \boldsymbol{T}_2^{\mathrm{f}}\boldsymbol{D}$, and $\boldsymbol{X}_{\mathrm{w}} = \boldsymbol{T}_1^{\mathrm{f}}\boldsymbol{X}$ are column vectors of size $(2M_0 + 1)$. The wave-domain secondary path $\boldsymbol{H}_{\mathrm{w}}$ is a square matrix of size $(2M_0 + 1) \times (2M_0 + 1)$ representing the coupling of the acoustic channels in the wave domain. In addition, we have the following conversion relationship [22],

$$\boldsymbol{H} = \boldsymbol{T}_2^{\mathrm{b}}\boldsymbol{H}_{\mathrm{w}}\boldsymbol{T}_1^{\mathrm{f}}, \quad \boldsymbol{H}_{\mathrm{w}} = \boldsymbol{T}_2^{\mathrm{f}}\boldsymbol{H}\boldsymbol{T}_1^{\mathrm{b}}. \tag{8}$$

3. WAVE-DOMAIN ANC WITH ONLINE SECONDARY PATH MODELLING

3.1. Diagonal Structure of $\boldsymbol{H}_{\mathrm{w}}$

A special property of the wave-domain secondary path $\boldsymbol{H}_{\mathrm{w}}$ as shown in Fig. 2 is that the matrix has dominant diagonal components [14, 15]. Especially, in mild to moderate reverberant environments, the matrix $\boldsymbol{H}_{\mathrm{w}}$ can be approximated as a diagonal matrix [16, 23]. A special case is for free-field sound propagation and ideal transducers, where $\boldsymbol{H}_{\mathrm{w}}$ is an identity matrix $\boldsymbol{I}$.

A more general representation of $\boldsymbol{H}_{\mathrm{w}}$ can be written as,

$$\boldsymbol{H}_{\mathrm{w}} = \boldsymbol{I} + \boldsymbol{\Gamma}, \tag{9}$$

where $\boldsymbol{\Gamma}$ represents only the reverberant part relative to the direct-path part in the wave domain. In a moderately reverberant environment, the non-diagonal entries of $\boldsymbol{\Gamma}$ have values much smaller than 1 and thus $(\boldsymbol{I} + \boldsymbol{\Gamma}_{\mathrm{diag}})$ becomes the dominant part of the matrix $\boldsymbol{H}_{\mathrm{w}}$.

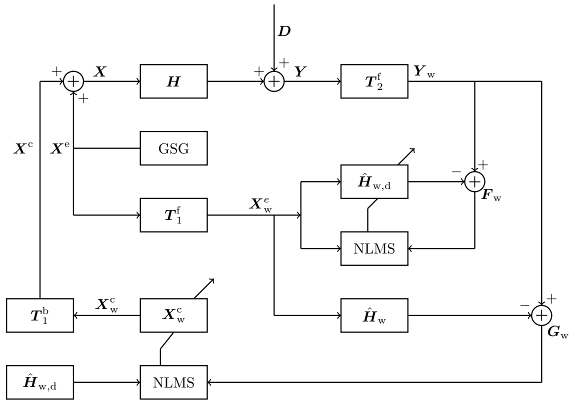

Fig. 3. Block diagram of wave-domain ANC with online SPM.

Our simulation results show that this diagonal structure holds as long as the loudspeaker array is not too close to a wall and the distance between the loudspeakers and microphones is not too large so that reverberation remains weaker than the direct-path component. This wave-domain acoustic channel property has been explored in the past for acoustic echo cancellation [24] and room equalization [15, 25] applications; next we will make use of it to develop a wave-domain ANC with online SPM.

3.2. Proposed System

The block diagram of the wave-domain ANC with online SPM is shown in Fig. 3. Referring to (2), there are two parts of the secondary source signals, $\boldsymbol{X}_{\mathrm{w}}^{\mathrm{c}}(q)$ and $\boldsymbol{X}_{\mathrm{w}}^{\mathrm{e}}(q)$ for ANC and SPM, respectively. The received microphone signals in the wave domain are represented as

$$\boldsymbol{Y}_{\mathrm{w}} = \boldsymbol{H}_{\mathrm{w}}(q)\big(\boldsymbol{X}_{\mathrm{w}}^{\mathrm{c}}(q) + \boldsymbol{X}_{\mathrm{w}}^{\mathrm{e}}(q)\big) + \boldsymbol{D}_{\mathrm{w}}(q). \tag{10}$$

The design of the proposed system is based on minimizing the following cost function,

$$\begin{aligned}\mathcal{J} &= \|\boldsymbol{Y}_{\mathrm{w}} - \hat{\boldsymbol{H}}_{\mathrm{w}}\boldsymbol{X}_{\mathrm{w}}^{\mathrm{e}}\|_2^2 \\ &= \|\boldsymbol{D}_w + \boldsymbol{H}_{\mathrm{w}}\boldsymbol{X}_{\mathrm{w}}^{\mathrm{c}} + \big(\boldsymbol{H}_{\mathrm{w}} - \hat{\boldsymbol{H}}_{\mathrm{w}}\big)\boldsymbol{X}_{\mathrm{w}}^{\mathrm{e}}\|_2^2. \end{aligned} \tag{11}$$

where $\hat{\boldsymbol{H}}_{\mathrm{w}}$ represents an estimate of the wave-domain secondary path.

In the following, adaptive algorithms are proposed to deal with time-varying noise and nonstationary acoustic environments. As pointed out in Sec. 3.1, for mild to moderate reverberant environments, $\hat{\boldsymbol{H}}_{\mathrm{w}}$ can be approximated as a diagonal matrix, which means different wave-domain components (or modes) can be considered independently of each other. In other words, the adaptive algorithms for estimating $\hat{\boldsymbol{H}}_{\mathrm{w}}$ and generating $\boldsymbol{X}_{\mathrm{w}}^{\mathrm{c}}$ can be designed as a parallel single-mode adaptation, i.e., an adaptation for each mode m, for $m = -M_0, \ldots, M_0$. This greatly reduces the computational complexity and leads to faster convergence as shown in the following.

Representing the system in matrix form, the update for online SPM is performed only on the diagonal part of the matrix $\hat{\boldsymbol{H}}_{\mathrm{w}}$, that is, a column vector $\hat{\boldsymbol{H}}_{\mathrm{w,d}} = \mathrm{diag}\{\hat{\boldsymbol{H}}_{\mathrm{w}}\}$ updated using the following equation

$$\hat{\boldsymbol{H}}_{\mathrm{w,d}}(q+1) = \hat{\boldsymbol{H}}_{\mathrm{w,d}}(q) + \mu_{\mathrm{e}}\frac{\boldsymbol{F}_{\mathrm{w}}(q) \circ \overline{\boldsymbol{X}_{\mathrm{w}}^{\mathrm{e}}(q)}}{\overline{\boldsymbol{X}_{\mathrm{w}}^{\mathrm{e}}(q)}\boldsymbol{X}_{\mathrm{w}}^{\mathrm{e}}(q) + \delta_e}, \tag{12}$$

where $\circ$ represents the Hadamard product (or element-wise product) of two matrices, $\overline{(\cdot)}$ denotes the conjugate transpose, and

$$\begin{aligned}\boldsymbol{F}_{\mathrm{w}}(q) &= \boldsymbol{Y}_{\mathrm{w}}(q) - \hat{\boldsymbol{H}}_{\mathrm{w},d}(q) \circ \boldsymbol{X}_{\mathrm{w}}^{\mathrm{e}}(q) \\ &= \big(\boldsymbol{H}_{\mathrm{w}}(q) - \hat{\boldsymbol{H}}_{\mathrm{w}}(q)\big)\boldsymbol{X}_{\mathrm{w}}^{\mathrm{e}} + \boldsymbol{D}_{\mathrm{w}}(q) + \boldsymbol{H}_{\mathrm{w}}(q)\boldsymbol{X}_{\mathrm{w}}^{\mathrm{c}}(q). \end{aligned} \tag{13}$$

As we assume one iteration per block, the time block index q also denotes the iteration step.

The anti-noise signals $\boldsymbol{X}_{\mathrm{w}}^{\mathrm{c}}$ are updated as follows,

$$\boldsymbol{X}_{\mathrm{w}}^{\mathrm{c}}(q+1) = \boldsymbol{X}_{\mathrm{w}}^{\mathrm{c}}(q) - \mu_{\mathrm{c}}\frac{\boldsymbol{G}_{\mathrm{w}}(q) \circ \overline{\hat{\boldsymbol{H}}_{\mathrm{w,d}}(q+1)}}{\overline{\hat{\boldsymbol{H}}_{\mathrm{w,d}}(q+1)}\hat{\boldsymbol{H}}_{\mathrm{w,d}}(q+1) + \delta_c}, \tag{14}$$

where

$$\begin{aligned}&\boldsymbol{G}_{\mathrm{w}}(q) = \boldsymbol{Y}_{\mathrm{w}}(q) - \hat{\boldsymbol{H}}_{\mathrm{w}}(q+1)\boldsymbol{X}_{\mathrm{w}}^{\mathrm{e}}(q) \\ &= \boldsymbol{D}_{\mathrm{w}}(q) + \hat{\boldsymbol{H}}_{\mathrm{w}}(q+1)\boldsymbol{X}_{\mathrm{w}}^{\mathrm{c}}(q) + \big(\boldsymbol{H}_{\mathrm{w}}(q) - \hat{\boldsymbol{H}}_{\mathrm{w}}(q+1)\big)\boldsymbol{X}_{\mathrm{w}}. \end{aligned} \tag{15}$$

The above two adaptation process influence each other. The signal properties of auxiliary noise $\boldsymbol{X}^{\mathrm{e}}(q)$ have great influence on the system performance. Here, we use a set of Gold sequences [26] that have extremely small cross-correlation within the set to generate $\boldsymbol{X}^{\mathrm{e}}(q)$ for online SPM. As the system is designed to cancel a single-frequency noise, $\boldsymbol{X}^{\mathrm{e}}(q)$ is generated using the ASK (Amplitude Shift Keying) modulation technique with the carrier frequency same as the noise frequency and the amplitude assigned by the Gold sequence generator (GSG). In addition, in this algorithm the step size (μ_{e} and μ_{c}) and regularization terms (δ_e and δ_c) are important parameters to tune for a stable system with fast adaptation performance and sufficient modelling accuracy.

4. EVALUATION

In this section, the setup and performance of the proposed ANC system with online SPM are described.

4.1. Experimental Setup

The experiments are performed in a simulated room environment which is generated using the image-source model [27]. The geometry of the experimental setup is shown in Fig.1, where the room has a size of 5×7 m and consists of four planar walls with the reflection coefficient β and perfectly-absorbing floor and ceiling. An 11-element loudspeaker array (blue) and an 11-element microphone array (red) with radii of 1.5 m and 0.5 m are concentrically placed at the point $(-0.5, 0.5)$ m relative to the room centre and used as the secondary sources and error sensors, respectively[1]. The primary noise source is located at $r = 2$ m, $\phi = 45^\circ$ with respect to the array centre and operates at the frequency of 500 Hz. The proposed method is also applicable to noise at other frequencies or multi-frequency noises as long as the number of secondary sources and error sensors meet the requirements. The loudspeakers and the noise source are modelled as 3D point sources. Furthermore, a sampling rate of 8 kHz is employed and the microphone recordings with 40 dB SNR are assumed.

[1]The number of loudspeakers and microphones are determined to satisfy the dimensionality requirement as shown in (5) and (6), that is given M_0 both L and P should be at least $2M_0 + 1$.

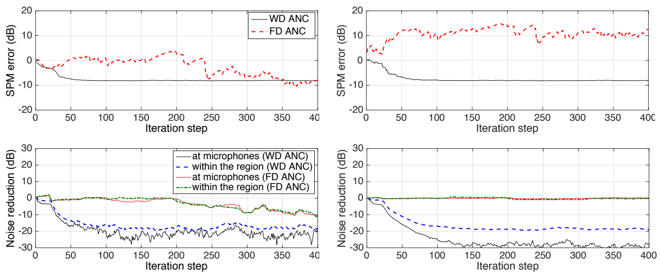

(a) (b)

Fig. 4. Adaptation performance of the proposed WD ANC compared with the conventional FD ANC. Plots correspond to different levels of auxiliary noise injected into the control region for online SPM, e.g., (a) 0.93 dB or (b) 12.97 dB lower than the primary noise level.

The system is evaluated by two objective measures, the SPM error and the noise reduction performance. The SPM error refers to the error between the estimated and the true channel of the multiple loudspeaker/multiple microphone setup. Noise reduction performance is investigated at the microphone positions as well as within the control region, as the aim of the system is to achieve noise reduction within a spatially extended 2D region.

4.2. Experimental Results

In the first experiment, the room is simulated with reverberation coefficient $\beta = 0.6$ and reverberation time $T_{60} \approx 170$ ms. The adaptation performance of the proposed wave-domain (WD) ANC system is plotted in Fig. 4, in comparison with the frequency-domain (FD) ANC system. Plots in Fig. 4 (a) and Fig. 4 (b) show the system performance with different levels of auxiliary noise injected for online SPM. In Fig. 4 (a), the auxiliary noise level is 0.93 dB lower than the primary noise level. This is the least amount of auxiliary noise required for online SPM of the FD ANC system to work. The proposed system however demonstrates much faster and more stable adaptation performance. In Fig. 4 (b), the auxiliary noise level is reduced to a very low level, which is 12.97 dB lower than the primary noise level. The proposed WD ANC converges after around 100 steps while the FD ANC fails completely.

Note that using the proposed system in both examples the SPM error is limited to -8.21 dB. This modelling error is mainly caused by not incorporating non-diagonal terms in $\hat{\boldsymbol{H}}_{\mathrm{w}}$; however, we can see that still a significant amount of noise reduction is achieved. In the FD ANC, the SPM error can decrease down to about -10 dB however at the expense of a significant increase of auxiliary noise level and computational complexity. For the example shown in Fig. 4 (b), Fig. 5 (a) plots the sound field generated by the proposed system after the system converges. As can be seen, a quiet zone is produced within the control region surrounded by the microphones. The energy of the original noise, auxiliary noise for SPM, and residual noise measured at the microphone in this example are plotted in Fig. 5 (b).

In summary, the above results in Figs. 4 and 5 show a clear advantage of modelling the WD secondary path as a diagonal matrix, that is instead of estimating the whole matrix as in FD ANC only the diagonal entries need to be estimated. This alleviates the well-known non-uniqueness problem in multichannel system identification [28] and allows adaptation with a much lower level of auxiliary noise.

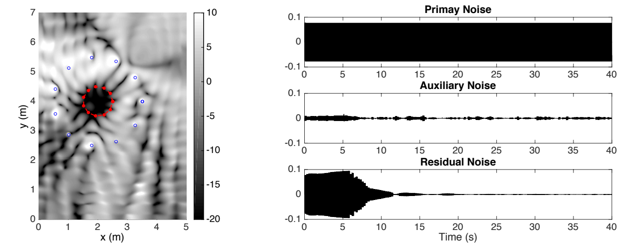

(a) (b)

Fig. 5. Plots are (a) the sound field generated by the proposed WD ANC after the system converges and (b) a comparison of the original noise, auxiliary noise for SPM and residual noise measured at the microphone.

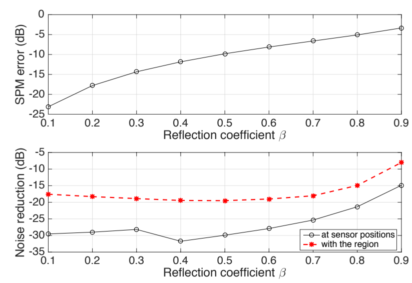

Fig. 6. Performance of the WD ANC under different reflection coefficients.

Figure 6 plots the system performance for different reverberant coefficients corresponding to the reverberation time T_{60} increasing from 110 to 570 ms. As the reflection coefficient β increases, the SPM error increases and the noise reduction performance drops as expected. The proposed WD ANC system with the assumption of modelling the WD secondary path as a diagonal matrix however is quite effective for mild to moderate reverberant environments. Even for the room with a high reflection coefficient $\beta = 0.9$ and a long reverberation time $T_{60} \approx 570$ ms, the SPM error reaches -3.34 dB, the noise reduction at microphones and within the region can still be kept at a reasonable level of -14.88 dB and -8.02 dB, respectively. To obtain better results for strong reverberation, one should include additional off-diagonal components as used by [25] for room equalization.

5. CONCLUSION

Adaptive wave-domain processing for multichannel ANC was presented in this paper to achieve online secondary path modelling and noise cancellation over a spatial region. Based on the dominant diagonal structure of the secondary path model in the wave domain, adaptive algorithms with reduced computational complexity and fast convergence speed were proposed. A feedback control strategy was adopted in the proposed system. Experimental results show that the proposed wave-domain ANC requires a much lower level of auxiliary noise for online secondary path modelling and achieves significant noise reduction over the entire design region.

6. REFERENCES

[1] C. C. Fuller, S. J. Elliott, and P. A. Nelson, *Active Control of Vibration*, Academic, San Diego, CA, 1996.

[2] S. M. Kuo and D. R. Morgan, “Active noise control: A tutorial review,” *Proceedings of the IEEE*, vol. 87, no. 6, pp. 943–973, 1999.

[3] H. Sano, T. Inoue, A. Takahashi, K. Terai, and Yoshio Nakamura, “Active control system for low-frequency road noise combined with an audio system,” *IEEE Trans. Speech Audio Process.*, vol. 9, no. 7, pp. 755–763, 2001.

[4] H. Chen, T. D. Abhayapala, and W. Zhang, “Spatial noise cancellation inside cars: Performance analysis and experimental results,” in *Proc. IEEE Workshop on Applications of Signal Processing to Audio and Acoustics (WASPAA)*, New Paltz, NY, Oct. 2015, p. 4 pages.

[5] S. J. Elliott, I. M. Stothers, and P. A. Nelson, “A multiple error lms algorithm and its application to the active control of sound and vibration,” *IEEE Trans. Acoust. Speech Signal Process.*, vol. ASSP-35, no. 10, pp. 1423–1434, 1987.

[6] T. Kosaka, S. J. Elliott, and C. C. Boucher, “A novel frequency domain filtered-x lms algorithm for active noise reduction,” in *Proc. IEEE International Conference on Acoustics, Speech, and Signal Processing (ICASSP)*, Munich, Germany, April 1997, vol. 1, p. 403406.

[7] S. C. Douglas, “Fast implementations of the filtered-x lms and lms algorithms for multichannel active noise control,” *IEEE Trans. Speech Audio Process.*, vol. 7, no. 4, pp. 454–465, July 1999.

[8] S. J. Elliott, C. C. Boucher, and P. A. Nelson, “The behavior of a multiple channel active control system,” *IEEE Trans. Signal Process.*, vol. 40, no. 5, pp. 1041–1052, 1992.

[9] Y. Kajikawa, W.-S. Gan, and S. M. Kuo, “Recent advances on active noise control: Open issues and innovative application,” *APSIPA Trans. Signal Inf. Process*, vol. 1, pp. 21 pages, August 2012.

[10] J. Zhang, W. Zhang, and T. D. Abhayapala, “Noise cancellation over spatial regions using adaptive wave domain processing,” in *Proc. IEEE Workshop on Applications of Signal Processing to Audio and Acoustics (WASPAA)*, New Paltz, NY, Oct. 2015, p. 4 pages.

[11] S. Spors and H. Buchner, “Efficient massive multichannel active noise control using wave-domain adaptive filtering,” in *Proc. International Symposium on Communications, Control and Signal Processing (ISCCSP)*, March 2008, pp. 1480–1485.

[12] J. Zhang, T. D. Abhayapala, P. Samarasinghe, W. Zhang, and S. Jiang, “Sparse complex FxLMS for active noise cancellation over spatial regions,” in *Proc. IEEE International Conference on Acoustics, Speech, and Signal Processing (ICASSP)*, Shanghai, China, March 2016, pp. 524–528.

[13] M. T. Akhtar, M. Abe, M. Kawamata, and A. Nishihara, “Online secondary path modelling in multichannel active noise control systems using variable step size,” *Signal Process*, vol. 88, no. 8, pp. 2019–2029, August 2008.

[14] H. Buchner, S. Spors, and W. Kellermann:, “Wave-domain adaptive filtering: acoustic echo cancellation for full-duplex systems based on wave-field synthesis,” in *Proc. IEEE International Conference on Acoustics, Speech, and Signal Processing (ICASSP)*, Montreal, Canada, May 2004, vol. 4, pp. 117–120.

[15] S. Spors, H. Buchner, and R. Rabenstein, “A novel approach to active listening room compensation for wave field synthesis using wave-domain adaptive filtering,” in *Proc. IEEE International Conference on Acoustics, Speech, and Signal Processing (ICASSP)*, Montreal, Canada, May 2004, number 4, pp. 29–32.

[16] M. Schneider and W. Kellermann, “A direct derivation of transforms for wave-domain adaptive filtering based on circular harmonics,” in *Proc. European Signal Processing Conference (EUSIPCO)*, Bucharest, Romania, August 2012, pp. 1034–1038.

[17] C. Hofmann and W. Kellermann, “Wave-domain transforms for irregular loudspeaker array topologies,” in *Proc. DAGA*, Nürnberg, Germany, March 2015, pp. 1606–1609.

[18] A. Kuntz, *Wave field analysis using virtual circular microphone arrays*, Ph.D. dissertation, Friedrich-Alexander University Erlangen-Nürnberg (FAU), June 2008.

[19] M. Schneider and W. Kellermann, “Multichannel acoustic echo cancellation in the wave domain with increased robustness to nonuniqueness,” *IEEE Trans. Audio, Speech, and Language Process.*, vol. 24, no. 3, pp. 518–529, March 2016.

[20] E. G. Williams, *Fourier Acoustics: Sound Radiation and Nearfield Acoustical Holography*, Academic Press, San Diego, CA, 1999.

[21] M. Schneider and W. Kellermann, “A wave-domain model for acoustic MIMO systems with reduced complexity,” in *Proc. IEEE Workshop on Hands-free Speech Communication and Microphone Arrays (HSCMA)*, Edinburgh, UK, May 2011, pp. 133 – 138.

[22] C. Hofmann and W. Kellermann, “Generalized wave-domain transforms for listening room equalization with azimuthally irregular spaced loudspeaker arrays,” in *Proc. IEEE International Conference on Acoustics, Speech, and Signal Processing (ICASSP)*, Shanghai, China, March 2016, pp. 594–598.

[23] D. Talagala, W. Zhang, and Abhayapala. T.D., “Active acoustic echo cancellation in spatial sound field reproduction,” in *Proc. IEEE International Conference on Acoustics, Speech, and Signal Processing (ICASSP)*, Vancouver, Canada, May 2013, pp. 620–624.

[24] D. Talagala, W. Zhang, and Abhayapala. T.D., “Efficient multichannel adaptive room compensation for spatial soundfield reproduction using a modal decomposition,” *IEEE Trans. Audio, Speech, and Language Process.*, vol. 22, no. 10, pp. 1522–1532, Oct. 2014.

[25] M. Schneider and W. Kellermann, “Adaptive listening room equalization using a scalable filtering structure in the wave domain,” in *Proc. IEEE International Conference on Acoustics, Speech, and Signal Processing (ICASSP)*, Kyoto, Japan, March 2012, pp. 13–16.

[26] D. V. Sarwate and M. B. Pursley, “Crosscorrelation properties of pseudorandom and related sequences,” *Proceedings of the IEEE*, vol. 68, pp. 593–619, May 1980.

[27] J. Allen and D. Berkley, “Image method for efficiently simulating small-room acoustics,” *J. Acoust. Soc. Am.*, vol. 65, no. 4, pp. 943–950, 1979.

[28] J. Benesty, D. Morgan, and M. Sondhi, “A better understanding and an improved solution to the specific problems of stereophonic acoustic echo cancellation,” *IEEE Trans. Speech Audio Process.*, vol. 6, no. 2, pp. 156–165, March 1998.